Egyptian Journal of Pure and Applied Science

Predicting Fundamental Transverse Electric Mode of Slab Waveguide Based on Physics-Informed Neural Networks

Omar E. Elsheikh[1,3], Adel Shaaban [2], A. Arafa [2], Ashraf Yahya[3], and Lotfy Rabeh Gomaa [5], Nasr Gad [3,4]

[1] Department of Physics, School of Sciences and Engineering, American University in Cairo, New Cairo 11835, Egypt

[2] National Center for Radiation Research and Technology (NCRRT), Egyptian Atomic Energy Authority Cairo, Egypt

[3] Electronics Group, Physics Department, Faculty of Science Ain Shams University Cairo, Egypt

[4] Department of Physics, Faculty of Science, Galala University, New Galala City, 43511, Egypt

[5] Faculty of Engineering at Shobra, Banha University Cairo, Egypt.

ARTICLE INFO

ABSTRACT

Over the past few years, deep learning has proved to be an efficient and fast tool in many areas, particularly in the field of photonics. The design of integrated optical devices relies on optical waveguides which requires reliable and fast methods for determining the waveguide's characteristics before fabrication. In this work, the newly emerging paradigm of physics-informed neural networks (PINNs) is employed for analyzing and predicting the fundamental transverse electric (TE) mode and effective refractive index (η) of a slab waveguide. PINNs are particularly useful, as they are a data- and mesh-free method, solving the most critical problems of computational modeling, such as speed and computational hardware cost. The proposed model has a prediction accuracy of up to 99%, with the effective refractive index relative error ranging between 10^{-5} and 10^{-6}. The model results are validated against finite difference time domain method using Lumerical software and variational method.

1. Inrtoduction

Currently, Machine learning techniques have received a great deal of attention, especially, its promising subset deep learning. Deep learning has been used extensively in a variety of scientific and engineering fields, including device design [1,3], an inspection of electronic chips in semiconductor production lines [4], computer vision [5], and natural language processing and cognitive sciences [6]. There has also been a tremendous effort to use deep learning in the field of photonic devices, particularly in analyzing and predicting waveguide characteristics as in [7,10].

However, these works have used supervised learning – more or less - to accomplish great results which need to train the model on data with known input and output, this data needs to be prepared first before training the model, which may take time and resources. In this work, a suggested model was built to predict the characteristics of the waveguides without supervision and only know about the physics of the device through boundary conditions. The physics-informed neural network (PINN) has been proposed by Raissi et al [11] to fill the gaps between deep learning and solving differential equations that started in 1990 by Hyuke Lee [12], followed by Lagaris et al [13]. This work aims to demonstrate the applicability of PINNs based method to a well-known problem in the optical devices field to predict the fundamental transverse electric (TE) mode of the dielectric slab waveguide. On the other hand, the suggested method might be upgraded to predict the other modes.

The paper consists of seven sections; Section **2** describes the dielectric waveguide concepts, the modeling parameters, and techniques for analyzing waveguides. Section **3** defines the slab waveguide problem. Besides, Section **4** presents the fundamentals of the physics-informed neural network, the suggested method based on it, and the implementation details. Furthermore, section **5** shows the results of the suggested method. The interpretation of the results and impact of the proposed method on the field of photonics are discussed in section **6**. Finally, the paper is concluded in Section **7**.

2. Analyzing Waveguides

Over the past years, optical waveguides have been the basic elements for confining and transmitting light efficiently over various distances, ranging from tens or hundreds of micrometers in integrated photonics to hundreds or thousands of km in long-distance fiber-optic transmission [14,15]. Various structures of waveguides have been made, and the choice of these structures is governed by the desired frequency band, the amount of power to be transferred, and the amount of transmission losses that can be tolerated.

Optical waveguides also form a key element in semiconductor lasers, acting as both passive and active devices such as waveguide couplers and modulators [16]. There are two types of waveguides: metallic waveguides and dielectric waveguides [17], and in this article we are interested in the latter. Dielectric slabs are thin layers of high-index material, which may be referred to as films or cores, placed between two layers: the upper layer is called the cladding and the lower layer is called the substrate [18].

There are two types of dielectric waveguides: planar and non-planar. Planar waveguides consist of a core film with a higher refractive index than the substrate or the cladding. Symmetric waveguide designs are achieved when the cladding and substrate have the same refractive index, while anti-symmetric waveguides are obtained otherwise.

In any waveguide, two of the most important characteristics to be aware of are the propagating modes and the effective refractive index. A waveguide mode is a transverse field pattern whose amplitude and polarization profiles remain constant along the longitudinal z-coordinate. A guided mode can only exist when a transverse resonance condition is satisfied, such that the repeatedly reflected wave has constructive interference with itself. The effective index is the ratio of the propagation constant in the waveguide to the free space propagation constant, as in

$$N_{eff} = \frac{\beta\lambda}{2\pi} \tag{1}$$

Where, β is the propagation constant and λ is the free-space wavelength.

2.1. Techniques for analyzing waveguides

The electromagnetic fields propagating along the waveguide are composed of guided modes, also known as eigenmodes. These electromagnetic fields can be analyzed using three approaches: analytical, numerical, and the more recent, promising deep learning approach. The analytical solution is acquired by solving Maxwell's equations [19]. However, only simple waveguide geometries can be solved in this way [20]. However, only simple waveguide geometries can be solved in this way. For this reason, and due to the practicality of more complex waveguide geometries, the numerical approach has become the more appropriate choice.

Numerical methods are built upon approximations of the exact solution to the standard one, with the aim of minimizing the error between the two solutions [21]. There are various numerical methods available, such as the finite difference method (FDM) [22], finite element method (FEM) [23], method of lines (MoL) [24] and beam propagation method (BPM) [25] There are various numerical methods available, such as the finite difference method (FDM), finite element method (FEM), method of lines (MoL), and beam propagation method (BPM), which can be used to solve the eigenmode.

These methods have had great success in analyzing complex waveguide structures in recent years, leading to very established software in the field built upon these methods, such as Lumerical software [26], COMSOL software [27], among others.

However, these methods or software come with some sacrifices in terms of speed of analysis and computational resources used as waveguides become more complex. As for the deep learning approach, it has been reported to successfully design [28], predict modes [29,30] and properties of photonic waveguides. In all of the reported articles, they used what is known as "supervised learning", wherein the user has input variables (X) and an output variable (Y), and an algorithm is used to learn the mapping function from the input to the output.

The goal is to approximate the mapping function so well that when new input data (X) is presented, the output variables (Y) can be accurately predicted. Although these previous articles and others obtained very good predictions that were close to the results of numerical methods, and after training, the model can make its predictions in milliseconds, the data must first be prepared using numerical methods or software and preprocessed in order to be ready to train the deep learning model. Our proposal here is to use the capabilities of deep learning methods to predict the TE mode and N_{eff} of a slab waveguide when no prior knowledge about it is available to the model. This falls under the type of deep learning called "unsupervised learning", wherein only input data (X) is available and no corresponding output variables.

The goal of unsupervised learning is to model the underlying structure or distribution in the data, governed by certain constraints (in our case, boundary conditions), in order to learn more about the data. Since waveguides are physical systems governed by physical laws, we need a model to be guided by not just random statistical methods, but also with physics constraints. In other words, we want to empower the deep learning model with known physical laws. Raissi et al. [11] presented what is called physics-informed neural networks (PINNs), which intend to solve inverse and direct problems by different types of partial differential equations (PDEs).

The loss function of a PINN consists of several terms, including different governing equations and boundary conditions. In particular, the training data used by this framework can be provided by a sample within the domain of definition of the problem itself, without needing to generate data as in a supervised approach. PINNs have been used successfully in many fields to solve PDEs, such as material science [31], fluid mechanics [32]. In this paper, we aim to predict the characteristics of a waveguide by solving its eigenvalue problem with the help of PINNs. Our intention is not to replace the conventional solutions for eigenvalue problems, but to demonstrate the power and effectiveness of neural networks in the future of waveguide design and the field of photonics in general.

3. Slab Waveguide Problem Definition

Consider a slab waveguide as in Fig. 1. It consists of a film region with thickness h and refractive index n_f, sandwiched between cladding and substrate with refractive indices n_c and n_f respectively.

The three indices are chosen such that n_f is bigger than n_c and n_s in order for total internal reflection to occur at the interfaces [33]. If the cover and substrate materials have the same index of refraction, the waveguide is called "symmetric", otherwise the waveguide is called "asymmetric". The symmetric waveguide is a special case of the asymmetric waveguide. Conventionally we take z-axis is the direction of propagation for electromagnetic field. There are two possible electric field polarization, transverse electric (TE) or transverse magnetic (TM). As a special case, we restrict our analysis to TE modes, which have $E_z = 0$. In the TE case, the E-field is polarized along the y-axis. We assume that the waveguide is excited by a source with frequency ω_0 and a vacuum wave vector of magnitude $k_o = \omega_0/c$.

Now we have to solve the Helmholtz's wave equation in each dielectric region to find the allowed electric fields or modes, and then use the boundary conditions to connect these solutions. If Ω is the domain of the slab waveguide such that, $\Omega \in R$ then, Helmholtz equation becomes

$$\frac{\partial^2 E_y}{\partial x^2} + \frac{\partial^2 E_y}{\partial y^2} + \frac{\partial^2 E_y}{\partial z^2} + \left(k_0^2 \, n_i^2\right) E_y = 0$$

(2)

where $n_i = n_f, n_s, n_c$, depending on the location. If we assume that our slab waveguide is infinite in the y-direction and due to the translational invariance of the structure in the z-direction, we do not anticipate the amplitude to vary along the z-axis, but we do expect that the phase varies. So the trial solution for equation (2) will be

$$E_y(x, z) = E_y(x) \, e^{-j\beta z} \qquad (3)$$

Where β is a propagation coefficient along the z-direction, substitute this in equation (2), since

$$\frac{\partial^2 E_y}{\partial y^2} = 0$$

$$\frac{\partial^2 E_y}{\partial x^2} + \left(k_0^2 \, n_i^2 - \beta^2\right) E_y = 0 \qquad (4)$$

The objective of this study is to solve equation (4) for unknown field $E_y(x)$ and β which are eigen function and eigen value, respectively. The solution of this equation has two parts. The first part describes the solution for the cladding or substrate regions, where $\beta > k_0 n_i$, and has a real exponential form given b

$$E_y(x) = E_0 \, e^{\pm \sqrt{\beta - k0^2 \, n_i^2} \, x} \quad \text{for } \beta > k_0 \, n_i \qquad (5)$$
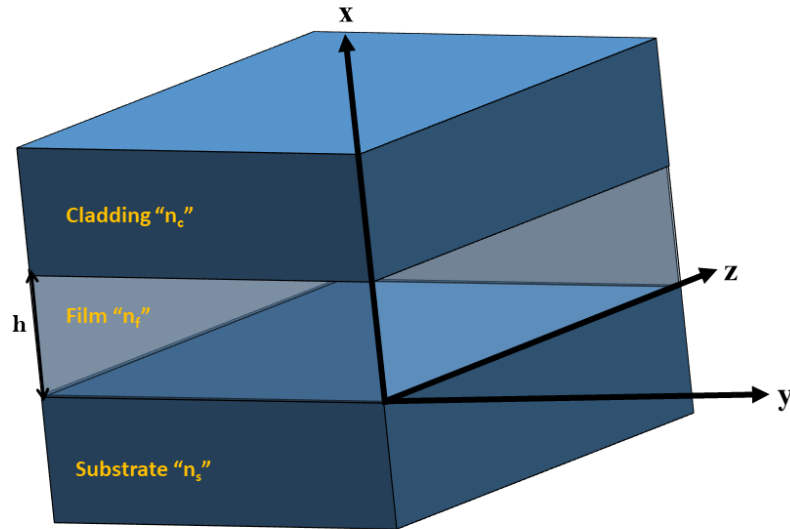
Fig. 1 The slab waveguide

Where E_0 is the field amplitude. The second part describes the solution for the core regions, where $\beta < k_0 n_i$ and the solution has an oscillatory form given by

$$E_y(x) = E_0 \, e^{\pm \sqrt{k0^2 \, n_i{}^2 - \beta} \, x} \quad \text{for } \beta < k_0 \, n_i$$

(6)

In other words, based on the value of β the solution can be either oscillatory or exponentially decaying. Therefore, the guided must satisfy the condition given by

$$k_0 \, n_s < \beta < k_0 \, n_f$$

(7)

To find the values of β that lead to allowed solutions or the eigen values to the wave equation, we must apply the boundary conditions to the general solutions developed in equation (5) and equation (6).

Assume that β satisfies equation (7). Then the transverse portions of the electric field amplitudes in the three regions are

$$E_y(x) = \begin{cases} A \, e^{-\sqrt{\beta - k0^2 \, n_i^2} \, x} & 0 < x \\ B \cos(k_f x) + C \sin(k_f x) & h < x < 0 \\ D \, e^{\sqrt{k0^2 \, n^2 - \beta}}(x + h) & x < -h \end{cases}$$

(8)

Where A, B, C and D are amplitudes coefficients that will be determined from boundary conditions. k_f is the transverse component of wavenumber k in the guiding film [33]. So when training the model, we have to make sure that we satisfy the boundary conditions to predict the eigen values and eigenvectors represented in our case from equation (4) as β and Ey, respectively. To achieve this we will use what Lagaris et al. proposed for solving PDEs.

4. The Suggested Physics-Informed Neural Network based method

The framework of PINNs is based on neural network and described in previous published work. The neural network unit is described as:

$$N_{W,b}(x) = \alpha \, (W * x + b)$$

(9)

Where W is a matrix and b is a vector represents weights and biases of neural network, x is the input vector to the network. α denotes the nonlinear activation function [34]. $W \in \mathbb{R}^{Nn}$, $b \in \mathbb{R}^{Nn * 1}$. The deep learning (DL) approach deals with more than one neural network, which form a multilayer neural network with linear output described as

$$u_\Theta(x) = W * (N_{\Theta_{L-1}} o \, N_{\Theta_{L-2}} o \dots o \, N_{\Theta_1(x)}) + b$$

(10)

$W^L \in \mathbb{R}^{N_L * N_{L-1}}$, $b^L \in \mathbb{R}^{N_L * 1}$. According to [35] who states that "A function neural network can approximate any smooth function arbitrarily close provided a sufficient number of neurons N_n. Consequently, the objective of a DL network is to estimate the value of u, Fig. **2** illustrates the PINNs-based solution's framework for solving the dielectric slab wave guide is shown. The left part shows the Fully Connected Neural Network, FNN(x, Θ) where $\Theta = \{W^l, b^l\}^L_{l=0}$. −

The FNN takes x as input to predict the solution E_y. This input represents a vector of points belong to the domain which dedicated for the waveguide, x ∈ [-x, x]. This domain should cover the waveguide from substrate to cladding including film regions. We have to choose the width of cladding and substrate wisely to give the propagated field enough space to decay outside the film region. Also we found that choosing appropriate domain will help to find the solution much faster. By applying chain rule, the derivatives of E_y with respect to inputs can be computed automatically [36].

Then the FNN can be learned through the parameters of Θ by minimizing the mean square error of the loss functions shown in

$$\text{Loss} = \overline{L_F^2 + L_e^2 + L_{bc}^2 + L_w^2}$$

$$(11)$$

Where,

$$L_F = \left[\frac{\partial^2 E_y}{\partial x^2} + \left(k_0^2 \, n_i^2 - \beta^2\right) E_y\right]^2 \qquad (12)$$

$$L_e = \left[e^{nc-Neff} - \left(e^{Neff-nc} + e^{ns-Neff}\right)\right]^2 \qquad (13)$$

$$L_{bc} = [\, u - u0\,]^2_{1,\partial\Omega} \qquad (14)$$

$$L_w = [\Theta_u]^2 \qquad (15)$$

Such that, u represent the function to optimize in equation (10). The first term in equation (11) is the fidelity term for the eigen function. The second term represents the eigen value loss. The third term imposes boundary conditions, and $\partial\Omega$ is the boundary. The final term is the conventional weight decay term which stabilizes the network weights. The total loss function is calculated by taking the average of all the losses components.

4.1. Implementation details

Our network is constructed as a fully connected network with a four-hidden-layer architecture, each layer containing a varying number of neurons from 30 to 80. We use PyTorch library [37] for our implementation. The Iterations varies between $5000 - 10,000$ according to the thickness and refractive indices of the waveguide, but we found that 10,000 iterations are enough to reach stability in our network for most tested cases. For NN optimization, the Adam optimizer [38] is used in our implementation, with its parameters set to the default. Our point set consists of 1000 training points and 100 boundary points.

5. Results

We will analyze a symmetric slab waveguide with the following parameters $n_c = n_s = 1.2, n_f = 1.3$, a film thickness of 0.5, and a wavelength of $\lambda = 1\,\mu m$. We could achieve the propagation constant $\beta = 7.766$ as in Fig. **3**. According to equation (1), the resultant effective refractive index is $N_{eff} = 1.23510549$, which is very close to the ground truth obtained from Finite difference method using FDTD [39] and variational method [40] with a relative error $1e^{-5}$.

Fig. **4** shows the predicted fundamental mode (TE mode) E_y with a relative error $1e^{-2}$. The training time ranges from 60 to 120 seconds, while predictions happen in milliseconds after the model finished training. There are some errors at the sides, which is a problem encountered when the model exponentially decays in the substrate and cladding; however, the matching in the core region and most parts of the sides are very close, indicating that the model has successfully predicted the TE mode, especially in the core region.

The proposed model has been tested over various symmetric and anti-symmetric waveguides with different refractive indices for each. Symmetric and anti-symmetric cases are represented in Tables **1**. and **2**., respectively. The proposed model achieved very high accuracy of 99% for predicting the propagation constant. Fig. **5** shows a relative error of predicting ranges between 10^{-5} and 10^{-6}. The green bars indicate waveguides with much variation between both cladding, substrate, and core, which results in two important observations in the simulation: first, as the spacing between the cladding, substrate, and core increases, the time taken for the model to find the right propagation constant increases; second, an increase in the margin between these three values leads to a decrease in the value of the propagation constant, resulting in a much lower error.
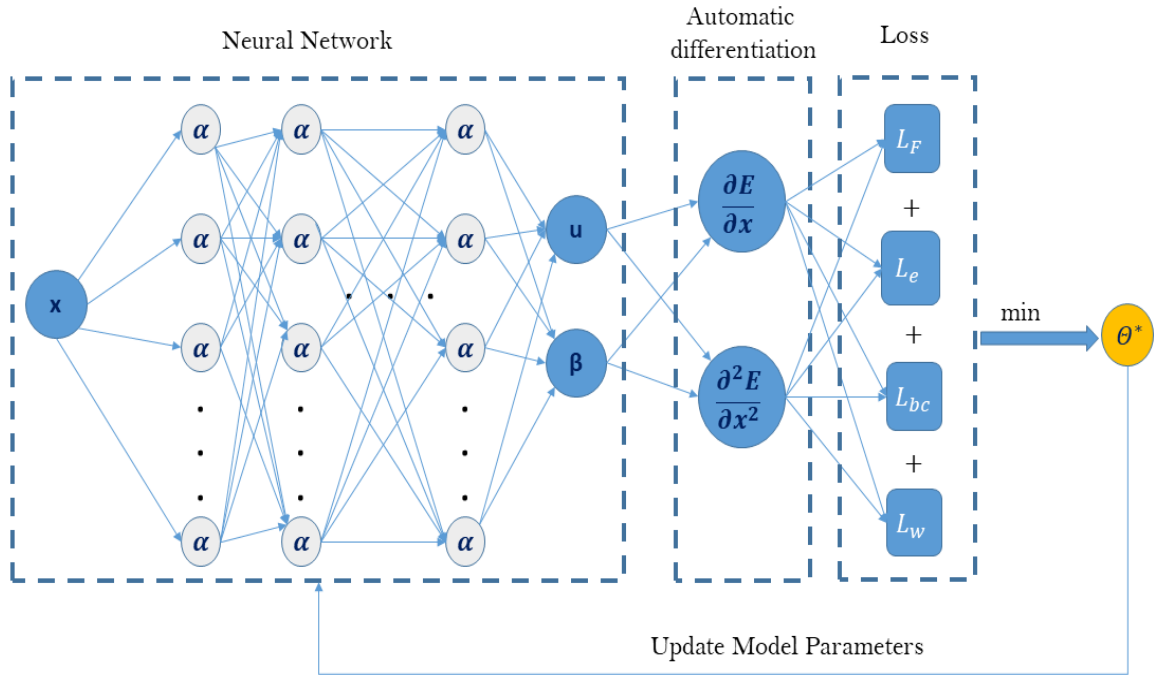
Fig. 2 Schematic of proposed PINNs for solving dielectric waveguide. The right most part represent the neural network layers with input x and two outputs, electric field and propagation constant. The left most part represent the loss factors.
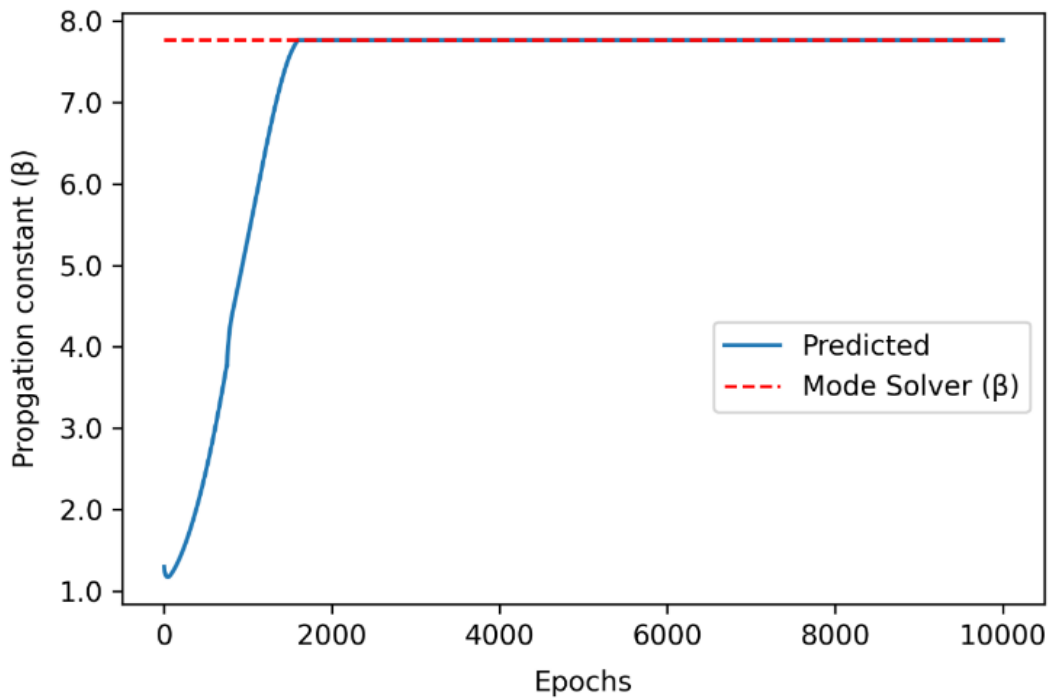

Fig.3 The propagation constant vs epochs compared to the calculated by mode solver (in case of symmetrical waveguide). The relative error of propagation constant is 10^{-5}.
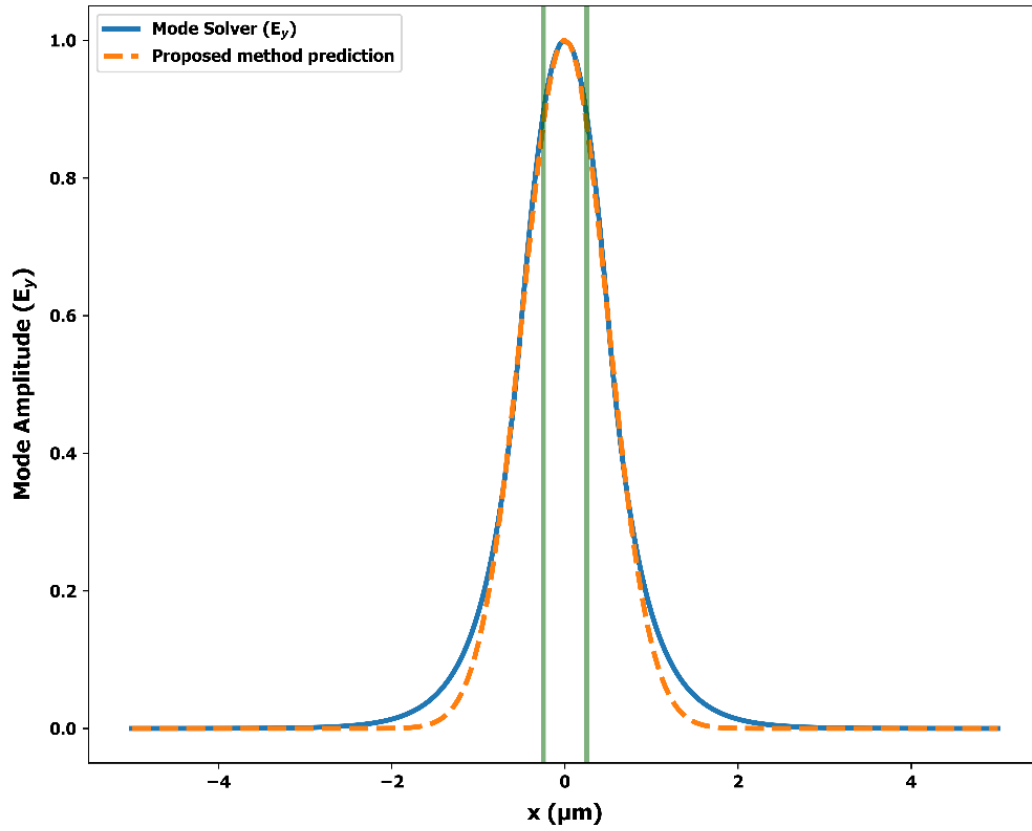
Fig. 4 The predicted fundamental mode for a symmetric waveguide compared to the calculated using mode solver. The calculated relative error of the mode profile (E_y) is 10^{-2}.
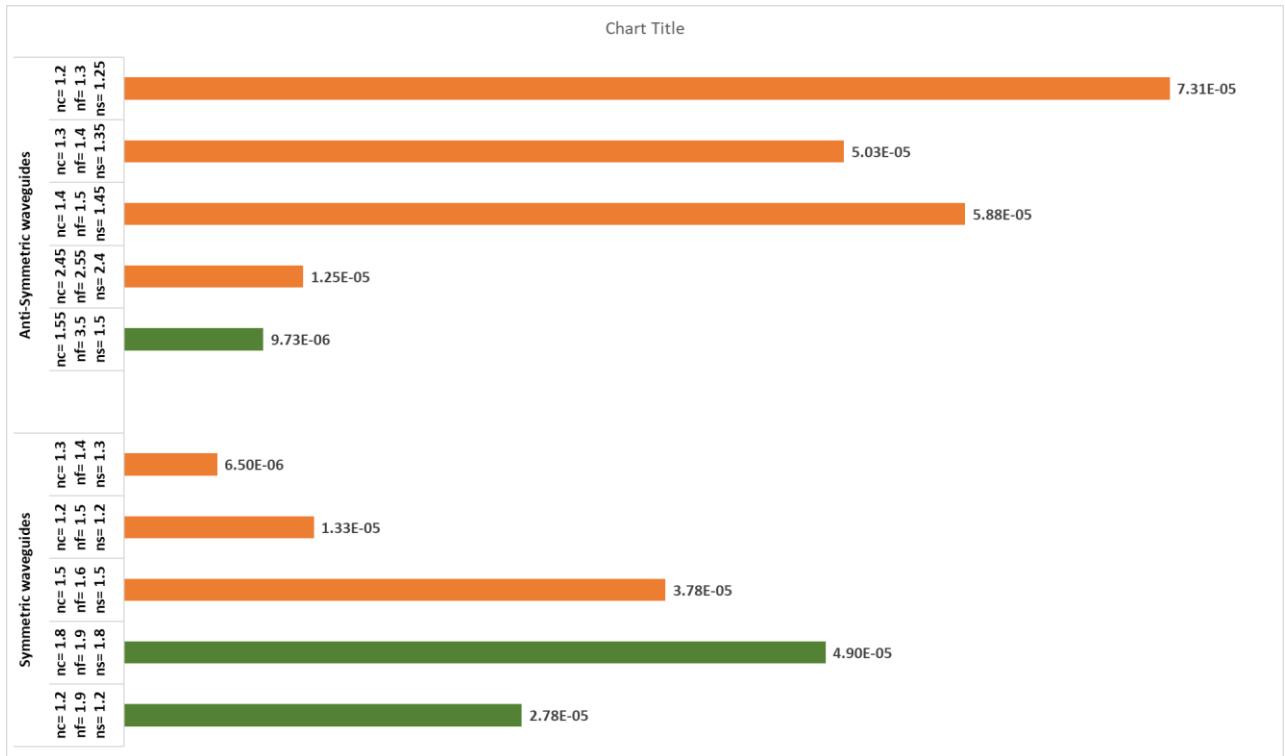

Fig. 5 Predicted N_{eff} error (from **Table 1.** and **Table 2.**) over different waveguide structures

Table 1. Data and Accuracy for Symmetric waveguides

	Waveguide Parameters	Numerical Propagation constant (βeta) from Lumerical[26]	Predicted Propagation constant (βeta)	Numerical effective refractive index from Lumerical[26]	Predicted effective refractive index	Accuracy of DL model (Predicting βeta) %	RELATIVE ERROR (N_{EFF})
WG1	n_clad: 1.3 n_core: 1.4 n_sub: 1.3	8.40362314	8.40364647	1.33746946	1.33746946	99.999722	6.50478E-06
WG2	n_clad: 1.5 n_core: 1.6 n_sub: 1.5	9.6781004	9.67789268	1.54025924	1.54025924	99.997854	3.78364E-05
WG3	n_clad: 1.8 n_core: 1.9 n_sub: 1.8	11.5864674	11.58618927	1.84395313	1.84395313	99.9976	4.90335E-05
WG4	n_clad: 1.2 n_core: 1.5 n_sub: 1.2	8.72670695	8.72682667	1.38891697	1.38891697	99.998628	1.32623E-05
WG5	n_clad: 1.2 n_core: 1.9 n_sub: 1.2	11.1235727	11.12366867	1.7704208	1.7704208	99.999138	2.77964E-05

Table 2. Data and accuracy for Anti-symmetric waveguides

	Waveguide Parameter	Numerical Propagation constant (beta) from Lumerical[26]	Predicted Propagation constant (βeta)	Numerical effective refractive index from Lumerical[26]	Predicted effective refractive index	Accuracy of DL model (Predicting βeta)	Relative Error (N_{eff})
WG1	n_clad: 1.2 n_core: 1.3 n_sub: 1.25	7.87668759	7.87668759	1.25361376	1.25352216	99.99292178	7.30767E-05
WG2	n_clad: 1.3 n_core: 1.4 n_sub: 1.35	8.50934836	8.50934836	1.35430485	1.35437298	99.99473806	5.03063E-05
WG3	n_clad: 1.4 n_core: 1.5 n_sub: 1.45	9.14197757	9.14197758	1.45499092	1.45507646	99.99389032	5.87907E-05
WG4	n_clad: 2.45 n_core: 2.55 n_sub: 2.4	9.77454734	15.67880255	1.55566752	2.49539018	99.99852236	1.25232E-05
WG5	n_clad: 1.55 n_core: 3.5 n_sub: 1.5	10.40703934	21.36351863	1.65633175	3.40014267	99.99879881	9.7291E-06

6. Discussion

This paper presents an analysis of the effective indices of slab waveguides with very high accuracy, as demonstrated in Tables 1 and 2. The model achieved an accuracy of 99%, taking between 60 and 120 seconds to reach stability during the training phase. After training, the model can provide predictions in milliseconds with relative error ranges between 10^{-5} and 10^{-6}. This accuracy was found to be comparable to other popular and commercial software used in the integrated photonics industry.

The results of the analysis of the symmetric slab waveguide provide a strong indication of the accuracy and efficiency of the proposed model. This model is capable of providing accurate predictions in a short amount of time, making it beneficial for those seeking to use it in real-time applications. Additionally, the model can be applied to a variety of waveguide designs, allowing for faster and more accurate predictions in many scenarios.

7. Conclusion

Our experiments have demonstrated the capabilities of PINNs to solve the slab waveguide problem, achieving very good accuracy for its propagation constant and effective refractive index of 99% and 10^{-6}, respectively for its transverse electric mode. The model shows promising results for simple structures, such as slab waveguides, and can be extended in future work to solve complex structures.

The main aim of this study is to present an alternative approach that can be developed to solve the main problems of analyzing photonic structures: speed and computational cost. We hope that this work will motivate other researchers in the field of photonic devices to create a more efficient tool, with fewer steps and less time than the conventional methods, in the near future.

8. References

1. **Kojima K., Wang B., Kamilov U., Koike-Akino T., and Parsons K. (2017).** Acceleration of FDTD-based inverse design using a neural network approach. in *Optics InfoBase Conference Papers* vol. Part **F52-I.**

2. **Rivenson Y. *et al*. (2017).** Deep learning microscopy. Optica **4**, **1437.**

3. **Sinha A., Lee J., Li S., and Barbastathis G. (2017).** Lensless computational imaging through deep learning. Optica **4**, **1117.**

4. **Bai X., Fang Y., Lin W., Wang L., and Ju B. F. (2014).** Saliency-based defect detection in industrial images by using phase spectrum. IEEE Trans. Ind. Informatics **10, 2135–2145.**

5. **Krizhevsky A., Sutskever I., and Hinton G. E. (2017).** ImageNet classification with deep convolutional neural networks. *Commun. ACM* **60, 84–90.**

6. **Lake B. M., Salakhutdinov R., and Tenenbaum J. B. (2015).** Human-level concept learning through probabilistic program induction. Science **(80-.). 350, 1332–1338.**

7. **Alagappan G., and Png C. E. (2021).** Prediction of electromagnetic field patterns of optical waveguide using neural network. Neural Comput. Appl. **33, 2195–2206.**

8. **Gao B., Woo W. L., Tian G. Y. and Zhang H. (2016).** Unsupervised Diagnostic and Monitoring of Defects Using Waveguide Imaging with Adaptive Sparse Representation. IEEE Trans. Ind. Informatics **12, 405–416.**

9. **Liu A. et al. (2018).** Analyzing modal power in multi-mode waveguide via machine learning. Opt. Express **26, 22100.**

10. **Chugh S., Gulistan A., Ghosh S., and Rahman B. M. A. (2019).** Machine learning approach for computing optical properties of a photonic crystal fiber. *Opt. Express* **27, 36414.**

11. **Raissi M., Perdikaris P., and Karniadakis G. E. (2019).** Physics-informed neural networks: A deep learning framework for solving forward and inverse problems involving nonlinear partial differential equations. J. Comput. Phys. **378, 686–707.**

12. **Lee H., and Kang I. S. (1990).** Neural algorithm for solving differential equations. *J. Comput. Phys.* **91, 110–131.**

13. **Lagaris I. E., Likas A., and Fotiadis D. I. (1998).** Artificial neural networks for solving ordinary and partial differential equations. IEEE Trans. Neural Networks **9, 987–1000.**

14. **Orfanidis S. J. (2005).** Waves and Antennas Electromagnetic. Media 2, 687–688 (2008).

15. Liu, J. M. Photonic devices. Photonic Devices vol. **9780521551**

16. **Agrawal G. P. (2002).**Fiber-Optic Communication Systems. Fiber-Optic Communication Systems **doi:10.1002/0471221147.**

17. **Okamoto K. (2006).** Fundamentals of Optical Waveguides. Fundamentals of Optical Waveguides **doi:10.1016/B978-0-12-525096-2.X5000-4.**

18. **Doerr C. R., and Kogelnik H. (2008).** Dielectric waveguide theory. Journal of Lightwave Technology vol. **26 1176–1187** at **https://doi.org/10.1109/JLT.2008.923632**

19. **Clarricoats P. J. B. (1967).** Foundations for Microwave Engineering. Electron. Power **13, 29**

20. **Kawano K., and Kitoh T. (2001).** Introduction to Optical Waveguide Analysis. Introduction to Optical Waveguide Analysis **doi:10.1002/0471221600.**

21. **Ismail M. M., and Zainudin M. N. S. (2011).** Numerical method approaches in optical waveguide modeling. in Applied Mechanics and Materials vols. **52-54 2133–2137**

22. **Kunz K. S., and Luebbers R. J. (2018).** The Finite Difference Time Domain Method for Electromagnetics. The Finite Difference Time Domain Method for Electromagnetics **doi:10.1201/9780203736708.**

23. **Jin J.-M. (2014).** The Finite Element Method in Electromagnetics, 3rd edition. J. Chem. Inf. Model. **380**

24. **Gu J. S., Besse P. A., and Melchior H. (1991).** Method of Lines for The Analysis of The Propagation Characteristics of Curved Optical Rib Waveguides. IEEE J. Quantum Electron. **27, 531–537**

25. **Van Roey J., van der Donk J., and Lagasse P. E. (1981).** BEAM-PROPAGATION METHOD: ANALYSIS AND ASSESSMENT. J. Opt. Soc. Am. **71, 803–810**

26. Lumerical Inc. No Title. at **https://www.lumerical.com/.**

27. COMSOL Multiphysics®. No Title. at **https://www.comsol.com/.**

28. **Anika N. J., and Mia M. B. (2021).** Design and analysis of guided modes in photonic waveguides using optical neural network. Optik (Stuttg). **228.**

29. **Liu A. *et al*. (2018).** Analyzing modal power in multi-mode waveguide via machine learning. Opt. Express **26, 22100.**

30. **Alagappan G., and Png C. E. (2019).** Modal classification in optical waveguides using deep learning. J. Mod. Opt. **66, 557–561.**

31. **ButlerK. T., Davies D. W., Cartwright H., Isayev O., and Walsh A. (2018).** Machine learning for molecular and materials science. Nature vol. **559 547–555** at **https://doi.org/10.1038/s41586-018-0337-2**

32. **Brenner M. P., Eldredge J. D., and Freund J. B. (2019).** Perspective on machine learning for advancing fluid mechanics. Phys. Rev. Fluids **4.**

33. **Pollock C. R., and Lipson M. (2003).** Rectangular Dielectric Waveguides. in Integrated Photonics **99–123 doi:10.1007/978-1-4757-5522-0_5.**

34. **Goodfellow I., Bengio Y., and Courville A. (2016).** Deep learning Bible. Healthc. Inform. Res. **22, 351–354.**

35. **Hornik K. (1991).** Approximation capabilities of multilayer feedforward networks. Neural Networks **4, 251–257.**

36. **Baydin A. G., Pearlmutter B. A., Radul A. A., and Siskind J. M. (2015).** Automatic Differentiation in Machine Learning: A Survey. J. Mach. Learn. Res. **18, 1–43.**

37. **Paszke A. *et al.* (2019).** PyTorch: An imperative style, high-performance deep learning library. in Advances in Neural Information Processing Systems vol. **32.**

38. **Kingma D. P., and Ba J. L. Adam (2015).** A method for stochastic optimization. in 3rd International Conference on Learning Representations, ICLR 2015 - Conference Track Proceedings**.**

39. **MATLAB. (2021).** Matlab 2020. MathWorks Inc. **1**

40. **Hammer M.** 1-D mode solver for dielectric multilayer slab waveguides.